www.gondwanags.org.in
Research Article

ISSN : 2455-1953
JGSR
Journal of Geosciences Research
Vol. 10, No.1, January, 2025, pp. 14-21
Copyright © 2025, Gondwana Geological Society, Nagpur
All rights reserved

Appraisal of a Complex Landslide at Kohima Town, Nagaland, India

Notoka K.[1], C. Nokendangba Chang[1], Meripeni Ezung[2], Glenn T. Thong[1], Vishezhonu Kirha[1], Kelevinuo Dzuvichu[1], Kethongunuo Miachieo[1] and Temsulemba Walling[1*]

[1]*Department of Geology, Nagaland University, Kohima Campus, Meriema- 797004(NL), India*
[2]*Department of Physics, Kohima Science College, Jotsoma- 797002(NL), India*
*(*Corresponding Author, E-mail: temsuwalling@nagalanduniversity.ac.in; ORCID: 0000-0001-8406-9686)*

Abstract

The interplay between geological and geomorphic conditions, moisture significantly influence landslide occurrences, though their precise relationships are often inadequately defined. This study aims to elucidate the factors affecting landslide activity in the Tarliedzü area of Kohima town. The area has experienced surface instabilities very frequently for the last three decades disrupting traffic and causing severe hardships to many towns and villages of Nagaland. Several attempts to stabilize this chronic landslide by simple rock and soil fill in the depressed portions, erecting gabion, and retaining walls have failed to arrest the problem. The difficulty in finding a permanent solution stems from the fact that several geological factors are at play in tandem, hence making it a complex slide, which requires a pragmatic mitigation approach based on the findings of a multi-disciplinary approach. A comprehensive, multi-parameter analysis was therefore conducted, incorporating geological and geotechnical, kinematic studies, joint analyses, and resistivity surveys to identify the underlying causes of the landslides. The area consists of fractured shales and weathered layers with high water concentrations. Structurally, the rocks are intersected by 3-4 joint sets, which are well illustrated by rose diagrams and stereographic projections. These joints are responsible for a wedge or planar failure in these rocks. While geological discontinuities such as joints are critical contributors to slope instability, the inherent weakness of slope materials has further exacerbated the problem. High groundwater levels, as indicated in dug wells, also point to the saturation of subsurface materials, thereby accelerating the weathering of these weakened formations.

Keywords: Landslide, Kohima, Geotechnical Analyses, Kinematic Analyses, Resistivity Survey, Groundwater

Introduction

Slope failure is caused by increasing external stresses and material degradation (Zuoan *et al.*, 2006). Landslides have massive impacts on society, economy, and the environment. They are recurring phenomena in mountainous regions, especially during the monsoon. This is favored by terrain morphology, geology, climate, land use/land cover and anthropogenic factors. Due to a variety of geological factors, when hill slopes get steeper, a crucial stage may be reached, which makes them susceptible to failure at the first sign of stress, such as heavy rainfall. Land use practices and land cover have a direct or indirect impact on the stability of hill slopes because they regulate how quickly the underlying formations erode and weather. In tectonically active terrain, structures are crucial to instability, and rock masses on slopes are loosened by the erosional processes that cut through geologic formations. Slope materials have a direct impact on the occurrence of landslides. In some areas, rocks are extremely sheared and crumbled, which leads to rapid weathering. Rising groundwater tables due to percolating water into zones of sheared, crumbled, or crushed rocks cause a build-up of pore pressure that leads to slope instability.

Most landslides are complex phenomena, whose study necessarily requires a multidisciplinary approach, based on a wide range of observations, including geological and geomorphological mapping, geotechnical and geophysical investigations, geodetic surveys, and satellite and meteorological data analyses (Perrone *et al.*, 2006; Kawabata and Bandibas, 2009). Landslides commonly occur during the monsoon when water rapidly accumulates in the subsurface, resulting in a surge of pore water pressure in the soil. In addition to rainfall, soil moisture plays a vital role in the initiation of landslides (Alimohammadlou *et al.*, 2014; Bicocchi *et al.*, 2019; Song and Wang, 2019; Wei *et al.*, 2020). Generally, the probability of landslide occurrences is higher in terrain of higher elevation coupled with high slope angles (Suraj *et al.*, 2024). Beyond the immediate physical devastation, these occurrences cast an enduring economic and social impact on human habitats (Hong *et al.*, 2017). Different techniques are used to obtain useful information. Each technique allows the determination of specific triggering factors and/or physical features characterizing the landslide compared with the material not affected by the movement. Various geophysical

(Received : 20 September 2024 ; Revised Form Accepted : 05 December 2024)
https://doi.org/10.56153/g19088-024-0224-69

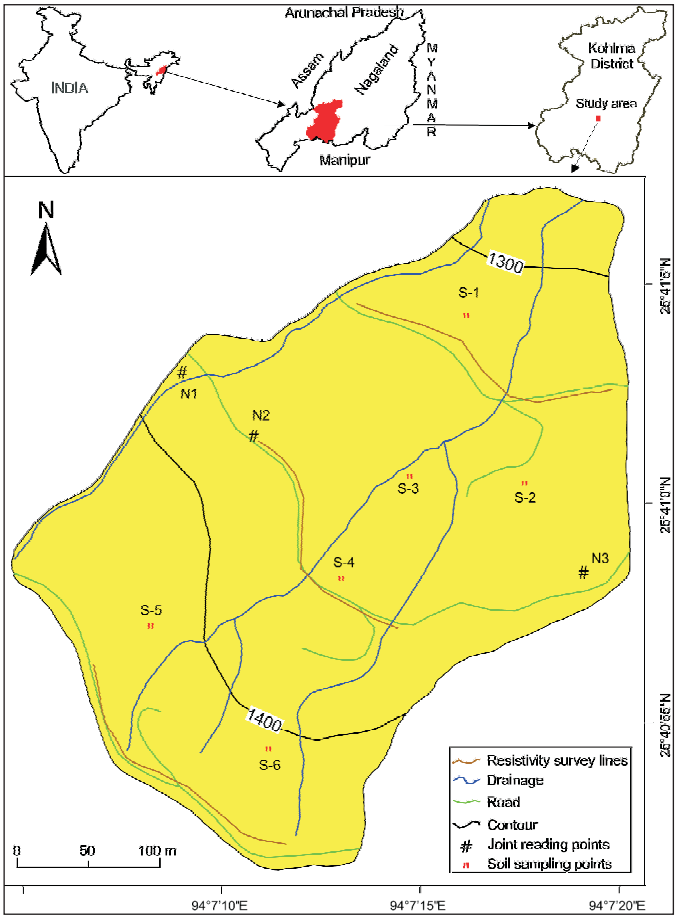

Fig.1. Location map of the study area

techniques (seismic, geoelectric, magnetometry, gravimetry, thermometry, GPS, *etc.*), which have led to significant results and provided useful information concerning both landslide-geometry reconstruction and site hydrological characterization (Jongmans and Garambois, 2007), can be applied to the investigation of landslides. Among these, the geoelectrical (electrical resistivity tomography, self-potential, induced polarization) and seismic methods play very important roles. In particular, the Electrical Resistivity Tomography (ERT) technique, based on the measurement of electrical resistivity values and their spatial distribution in the subsoil, has been largely applied to investigate landslide areas (Lapenna *et al.*, 2005; Godio *et al.*, 2006).

Kohima town occupies an area of about 17.5 sq km, with a population of 2,70,063 (Census of India, 2011). Kohima is considered tectonically unstable as it lies in Seismic Zone V, which is liable to seismic intensity of IX (Saikia and Arupjyoti, 2020). The Tarliedzü area, once considered a viable location for human habitation, is situated in the northeastern part of Kohima town (Fig. 1). This area has undergone dramatic changes due to landslide vulnerability in recent years. Decades back, the area hosted government quarters for the Industry and Commerce Department. However, persistent landslide activity severely damaged these structures (Fig. 2a). Much land in this area was therefore allotted to private parties. Since then, the area has seen a transformation with the landslide-affected zones in Tarliedzü characterized by a mix of kutcha (temporary) and some RCC (reinforced cement concrete) buildings. This evolving mix of construction types reflects the ongoing adaptation of the community to the challenging and unstable terrain. The lithology of the study area predominantly consists of shale with some silty shale (Fig. 2b-d). Numerous natural springs and open wells are noted in this area.

This paper aims to decipher the influence of geological and natural phenomena in causing the landslide events in the Tarliedzü locality by using various geological, geotechnical, and geophysical approaches to generate valuable data. This will help researchers in the region study the myriads of slope instabilities that are prevalent in north eastern India.

Study Area and Geological Setting

The Tarliedzü locality of Kohima town lies at latitudes 25°40'48"-25°41'08"N and longitudes 94°07'06"-94°07'18"E at an elevation of about 1440 m above mean sea level (Fig. 1). It is situated on the steep western limb of the Kohima Synclinorium, which is characterized by high hills and narrow valleys. The drainage systems are dominantly structurally controlled. An area of approximately 1,23,080 m^2 has been affected by numerous episodes of landslides during the last three decades, which has also severely affected National Highway-702A which passes through the study area. This highway connects Kohima to other districts. Several residential, commercial, and office buildings have been destroyed by surface instabilities.

Kohima town lies within the Inner Fold Belt of Nagaland and is composed of the Disang and Barail groups of rocks (Srivastava and Pandey, 2011). These rocks consist of shales, sandstones, and siltstones that are crumbled, crushed, and weathered to varying degrees due to the tectonic history of the area and the sub-tropical climatic conditions. Kohima receives >2800 mm of rainfall annually. The monsoon usually brings maximum precipitation. The region is part of the NE-SW trending Naga Hills, which in turn, are part of the northern extension of the rising IMR (Indo-Myanmar Ranges) of the Cretaceous-Tertiary orogeny (Morley *et al.*, 2020).

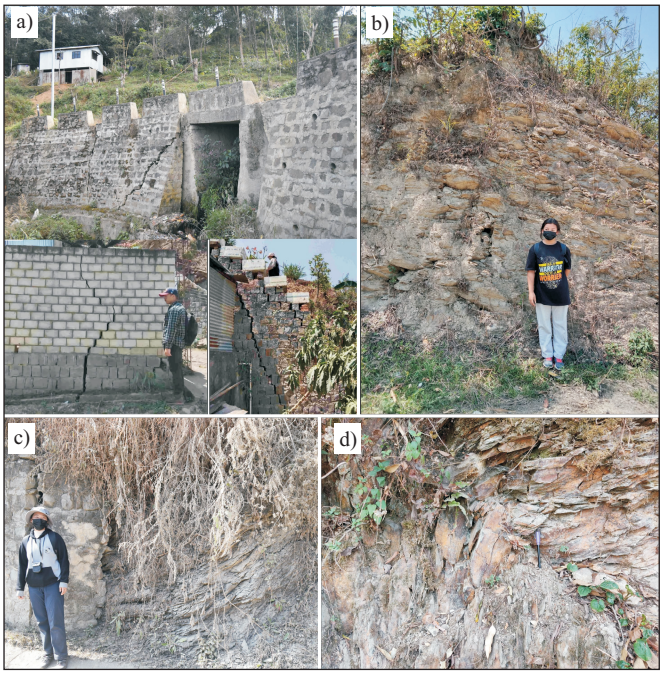

Fig.2. a) Tension fractures observed in structures indicating movement in the area, b) Crumbled weathered shale exposure in the area, c) Partially weathered shale in the study area, d) Disang shale intercalated with siltstone.

This is a comparatively young, immature mountainous setting. The tectonic displacement of the Indian Plate beneath the Burma Plate has resulted in significant elevation of the rocks of the region (Imchen *et al.*, 2014). The Cretaceous-era subduction and uplift are continuing (Verma, 1985; Nandy, 1976; Bhattacharjee, 1991; Aier *et al.*, 2011). This tectonically active region is characterized by significant shearing, faulting, fracturing, and widespread jointing of the rocks (Fig. 2b-d).

Methodology

Comprehensive field surveys and laboratory analyses were carried out to explore the relationship between slope geometry, lithology, and the structural characteristics in the landslide zone. Studies involved both field and laboratory testing of soil samples to assess their properties. During field surveys, geological discontinuities, including bedding planes, joints, and faults, were meticulously documented. A Brunton Compass was employed to measure the orientations of the exposed litho-units and structural features.

Structural data gathered from these surveys facilitated detailed kinematic studies to determine the movement and stability of the slopes. Resistivity surveys were conducted to probe subsurface conditions, thereby enhancing the overall understanding of the geological framework of the area and contributing to a more accurate assessment of landslide dynamics.

Geotechnical Analysis

Soil samples were systematically collected from six locations (S1-S6) within the study area for detailed geotechnical analyses (Fig. 1). Approximately 10 kg of soil was extracted using a trowel from trenches dug to depths of 1 meter. These samples were dried and processed according to ASTM D421 standards.

To determine the consistency limits of the soils, the samples were sieved through ASTM sieve no. 40 (425 µm), while shear strengths were assessed using fractions passing through sieve no. 10 (2 mm). Geotechnical analyses focused on evaluating three key consistency tests, the liquid limit, plastic limit, and shrinkage tests to measure changes in the behavior of soils with varying moisture contents.

The results of these tests were used to classify the soil types according to the Bureau of Indian Standards (1970) chart. This classification helps in the evaluation of the suitability of the soils where constructions are proposed, and their behavior under different environmental conditions. The cone penetrometer test, following the Bureau of Indian Standards (1985), was used to estimate the liquid limits of the soil samples. The plastic limit was determined using the rolling thread test, while the shrinkage limit was assessed through the immersion method in mercury following the Bureau of Indian Standards (1972).

For evaluating the shear strength of soils, direct shear tests were carried out to determine the cohesion (c) and internal friction angle (Φ) for remolded soil samples of the study area. The consolidated drained test method was conducted for the purpose following IS: 2720-13, 1986. The desired normal load in the range of 0.1 to 0.5 kg/cm^2 was applied through the loading frame. Readings were taken at intervals of 1 minute of shear displacement till failure. The sample was then removed and moisture content determined. Shearing was allowed at a low rate of constant strain (0.05 mm/minute) to permit complete drainage during shearing. The test was repeated with three more identical specimens under increased normal loads. Normal and peak shear stresses obtained from the tests were plotted in RocData software (Rocscience Inc., 2005) to obtain the cohesion (c), friction angle (Φ), and uniaxial compressive strength (σ_{ci}).

Slope Mass Rating

To estimate the stability conditions of the slopes, a slope mass rating was performed for the exposures in the study area (Romana, 1985) and the rock mass rating (RMR) of Bieniawski (1989). The rating values of the parameters of slope features, that is, the strength of intact rock, rock quality designation (RQD), discontinuity spacing and condition, and water input through discontinuities, were calculated to get the RMR. The RQD was estimated (Palmström, 1982) using the following equation:

$$RQD = 115 - 3.3J_v \quad (1)$$

where J_v - volumetric joint count (number of joints per unit length for all joint sets).

The strength of the rock was evaluated using a Point Load Index Tester in line with the Bureau of Indian Standards (1998). The following equation was used to translate the results of lump testing to UCS.

$$\sigma ci = K\,(PLI) \quad (2)$$

where K-conversion factor and PLI-point load index.

A conversion factor of 14.4 for shale was used after Singh *et al.* (2012). SMR was calculated using the following equation:

$$SMR = RMR + (F_1.F_2.F_3) + F \quad (3)$$

where F1, F2, and F3 - factorial adjustments of joint orientations with slope orientation and F4 - excavation method.

Joint trends were plotted in the Rocscience program (Dips Version 8.0) to construct a stereographic projection and a rose diagram. The potential modes of failure for the slopes were determined utilising characteristics such as dominant joint set, slope orientation, and internal friction angle for kinematic studies. RocData software (Rocscience Inc., 2005) was used to calculate friction angles. The input parameters include UCS, geological strength index (GSI), material constant of the rock (Mi), disturbance factor (D), unit weight of the rock, and slope heights. D is determined by the degree of disturbance experienced by the rock mass, such as blast damage or stress relaxation. It ranges from 0 for undisturbed, in-situ rock masses to 1 for highly disturbed rock masses. Since there was no blasting in the area, as the excavation was mechanical, the value assigned to D is 0.7 (Yang *et al.*, 2020).

Kinematic Analysis

The interactions between geological discontinuities such as joints, bedding planes, lineaments, and slope morphology are pivotal in elucidating the failure mechanisms prevalent on the slopes. Analysis of joint data in the field reveals the presence of two dominant joint sets. These joint sets, in conjunction with slope orientation, were used to construct a stereographic projection.

A stereographic projection is a fundamental analytical tool for structural geologists. It was meticulously developed using joint

attitudes to elucidate the structural behavior of the study area within its geodynamic context. This projection enabled a comprehensive assessment of slope failure types by visualizing the spatial relationships and interactions among the geological structures, thus providing an understanding of the underlying failure mechanisms.

Electrical Resistivity Analysis

A non-invasive geoelectrical resistivity approach was used to comprehend the subsurface better. Three survey lines, with a maximum current electrode separation of 120 m were chosen along the route, ensuring that the surveys followed straight lines and avoided conductors beneath the surface. The data was collected using a resistivity meter (Model number: SSR-MP-ATS Sl No. IGIS/18/20-21). The vertical electrical sounding (VES) resistivity variations method with the symmetrical Schlumberger configuration was used. Here, the current electrode spacing is greater than the potential electrode spacing by an order of 5 (AB/2 ≥ 5 MN/2; AB-current electrode spacing and MN-potential electrode spacing). The apparent resistivity 'ρ_a' of a geologic formation in a heterogeneous medium is the electrical characteristic variation with depth for a given electrode arrangement (Telford *et al.*, 1990).

$$\rho a = K\ \delta V/I \quad (4)$$

where $K = [\pi l/2] * [(L/l)^2 - 1]$, is the geometric spacing factor (AB = 2L; MN = 2*l*) with δV as the potential difference measured, and I as current induced into the ground.

The apparent resistivity value of the subsurface for each sounding is computed using equation (4) and then displayed as a digital value on the display screen of the resistivity meter. The field data were quantitatively analysed and interpreted using an interactive inversion code IPI2win (Bobachev, 2003) to determine the true resistivity.

Depending on resistivity values with depth, if ρ1, ρ2, and ρ3 are the resistivities of the subsurface layers, starting with ρ1 at the top and followed by ρ2 and ρ3, the four basic categories of sounding curve types may be summarised as follows (Orellana and Mooney, 1966):

ρ1<ρ2<ρ3: A-type
ρ1<ρ2>ρ3: K-type
ρ1>ρ2<ρ3: H-type
ρ1>ρ2>ρ3: Q-type

Results

Consistency Test

The natural moisture content of the six soil samples analyzed ranges from 11.35% to 32.81% (Table 1), which reflects the moisture conditions prevalent in the soils during the period of sampling. The average moisture content across these samples is 21.66 %.

The plasticity index (I_p) of the six soil samples ranges from 9.25% to 18.6%; such soils are moderate to highly plastic. Samples 2 and 6 exhibit a consistency index (I_c) of less than 1, which indicates very stiff soils. In contrast, samples 1, 3, 4, and 5 have I_c values exceeding 1, suggesting semisolid or solid-state conditions. These variations in plasticity and consistency indices provide a comprehensive understanding of soil behavior, highlighting differences in stiffness and plasticity across the sampled locations. The Plasticity limit determination is given in Table 2 and the Plasticity chart of the soil samples is in Fig. 3.

Table 1: Consistency limits of the soil samples

Sample no.	1	2	3	4	5	6
Natural moisture content (W_c)	17.94	30.56	19.93	11.35	17.41	32.81
Plastic limit (W_p)	20.62	28.4	23.52	17.82	33.75	32.36
Liquid limit (W_L)	38	47	37	29	43	48
Plasticity index (I_p)	17.38	18.6	13.48	11.18	9.25	15.64
Liquidity index (I_L)	-0.15	0.12	-0.27	-0.58	-5.83	0.46
Consistency index (I_c)	1.15	0.9	1.27	1.58	2.8	0.97
Shrinkage limit (S_L)	28.59	28.58	32.81	23.06	31.06	26.78
Degree of shrinkage (S_I)	4.11	13.09	2.80	4.79	8.64	12.44

Direct Shear Test of Soils

The values of cohesion and internal friction angles (Table 3) are obtained from the failure curves (Fig. 4). Samples show cohesion values ranging from 2-17kN/m^2, along slope angles 11°- 27°.

Slope Mass Rating

Slope mass rating (SMR) for locations N1 and N2 indicate Class III rocks, which are of fair quality. In contrast, location N3 falls in Class IV (Table 4), which indicates weak rock masses (Ramakrishna and Rajeshwara Rao, 2023).

Kinematic Analyses

Kinematic analyses were performed using 104, 68, and 80 joint attitudes from rock slopes N1, N2, and N3 respectively (Fig. 5a). Two dominant joint sets (J1, J2) have been identified in N1, one (J) in N2, and three (J1, J2, J3) in N3. On slope N1, joint sets J1 (70° due 100°) and J2 (70° due 351°) intersect to produce a wedge with a NE (43°) trend. In slope N2, the true dip of the joint plane (J=75°)

Table 2: Plasticity limit determination table

Group	Soil Sample	Soil type
CI	1, 3	Inorganic clay of medium compressibility and plasticity
CL	4	Inorganic clay of low compressibility and plasticity
MI/OI	2, 5, 6	Inorganic silt/very fine sand/ organic clay of medium compressibility and plasticity

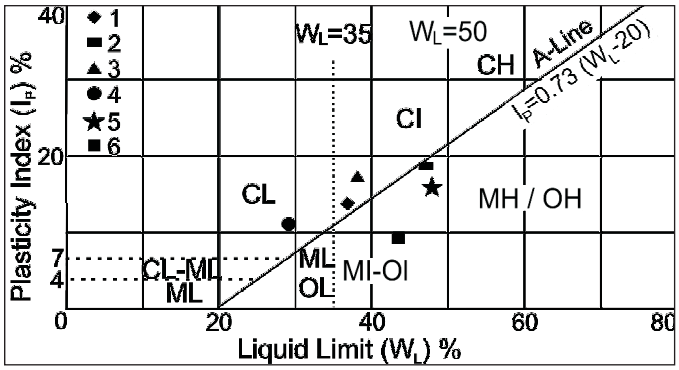

Fig.3. Plasticity chart of the soil samples (M - Inorganic silt/very fine sand; C -Inorganic clay; O - Organic silt/clay; L - Low compressible and plastic silt/clay; I- Medium compressible and plastic silt/clay; H - High compressible and plastic silt/clay)

Table 3: Shear strength parameters of the soil samples (UCS classification)

Sample	Cohesion (c)	Internal friction angle (Φ)	Uniaxial compressive strength
1	2.5	27	8.159 kN/m^2 = very weak
2	14	20	39.99 kN/m^2 = weak
3	2	23	6.043 kN/m^2 = very weak
4	2	18	5.506 kN/m^2 = very weak
5	3	18	8.258 kN/m^2 = very weak
6	17	11	41.25 kN/m^2 = weak

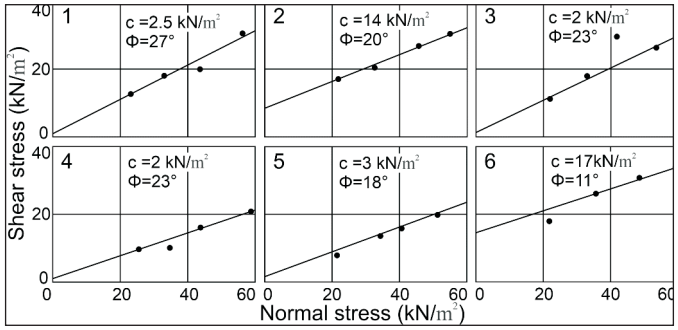

Fig.4. Failure curves of the soil samples

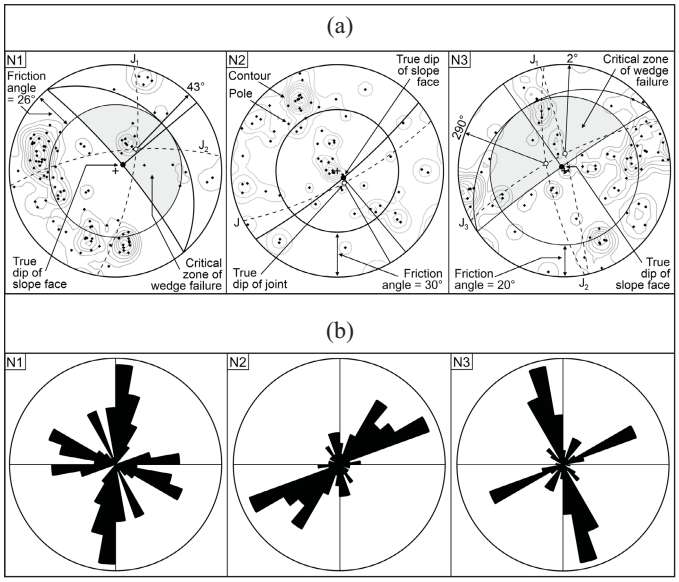

Fig.5. a) Stereographic projection, b) Rose diagram of the joints of the study area

lies at an angle of 5° with respect to the true dip of the slope face (80°). Here, the dip of the failure plane is less than the inclination of the slope and greater than the angle of friction (30°). The strike component of the joint plane (150°) and the slope face (140°) lies within ±10°.

Structural Analysis

The dominant geological trend observed at location 1 is NNE-SSW, which approximately corresponds to the regional fold and thrust directions. At location 2, the prevailing trend is NE-SW. In location 3, the dominant trend is NNW-SSE. Displacement along this direction has resulted in the development of sinistral strike-slip faults in the area (Fig. 5a-b).

Electrical Resistivity

The sounding curves of all VES exhibit curve types HKH, KH, and QH and show four to five geoelectric layers comprising the topsoil with layers of fractured shale, weathered to highly weathered shale, and shale with sandstone intercalations. The layer parameters for the VES points are given in Table 5.

Discussion

As moisture content increases, the consistency of soils transitions from stiffer conditions to fluid-like states, thereby decreasing their resistance to shear deformation. This parameter is crucial in the understanding of soil behavior under varying moisture

Table 4: Slope mass rating

Parameters	N1	Rating	N1	Rating	N3	Rating
1. UCS	19.90	2	25.67	4	18.98	2
2. RQD	-19.21%	3	3.79%	3	11.05%	3
3. Spacing of joints	63.24 mm	8	110mm	8	47.14mm	5
4. Condition of joints	Slightly rough surface. Separation<1mm; Slightly weathered	25	Slightly rough surface, separation <1mm. Highly weathered	20	Slightly rough surface, separation <1mm. Highly weathered	20
5. Groundwater condition	Dry	15	Completely dry	15	Damp	10
RMR	= (1+2+3+4+5)	53	= (1+2+3+4+5)	50	= (1+2+3+4+5)	40
6. $F_1 = (\alpha_j - \alpha_s)$	30	0.40	31	0.15	66	0.15
7. $F_2 = \beta_j$	72	1	74	1	67	1
8. $F_3 = \beta_j - \beta_s$ for plane failure						
$= \beta_j + \beta_s$ for toppling where β_s = dip/Angle of slope	-2	-50	0	-25	18	0
9. F_4= Adjustment factor	Pre-splitting	10	Pre-splitting	10	Pre-splitting	10
SMR=RMR + (F_1×F_2×F_3) + F_4	53+{0.40×1× (-50)}+10	43	50+{0.15×1×(-25)}+10	56.25	40+{0.15×1×(0)}+10	50
10. Class	III		III		III	
11. Description	Fair rocks; partially stable slopes		Fair rocks; partially stable slope		Fair rocks; partially stable slope	

Table 5: Layer parameters for the VES points

VES Station	Resistivity ρ (Ω m)	Thickness h (m)	Depth d (m)	Curve type	Inferred Lithology
1	ρ1 = 153	h1 = 4.97	d1 = 4.97	HKH	Topsoil/ shale exposures
	ρ2 = 50.3	h2 = 4.71	d2 = 9.68		Fractured shale
	ρ3 = 335	h3 = 9.45	d3 = 19.1		Shale with sandstone intercalations
	ρ4 = 26	h4 = 19.7	d4 = 38.8		Highly weathered shale/clay
	ρ5 = 4519	-	-		Undefined strata
2	ρ1 = 129	h1 = 6.7	d1 = 6.7	KH	Topsoil/ shale exposures
	ρ2 = 395	h2 = 3.87	d2 = 10.6		Shale with less moisture content or shale with sandstone intercalations
	ρ3 = 25	h3 = 8.43	d3 = 19		Fractured shale
	ρ4 = 11667	-	-		Undefined strata
3	ρ1 = 10000	h1 = 0.155	d1 = 0.155	QH	Topsoil/ shale with sandstone intercalation exposures
	ρ2 = 106	h2 = 9.37	d2 = 9.52		Fractured shale
	ρ3 = 26.5	h3 = 31.1	d3 = 40.6		Highly weathered shale/clay
	ρ4 = 12893	-	-		Undefined strata

conditions, which may range from a solid to semisolid, plastic, or liquid state, and the potential impact on slope stability. The average moisture content of 21.66% of the samples indicates that the soils possess relatively high natural moisture content. This elevated moisture content suggests a substantial water-holding capacity, which contributes to reduced shearing resistance and causes the soil to behave like liquids. The degree of shrinkage of samples 1, 3, and 4 points to less than 5% shrinkage values, which indicates they are good-quality soils with minimal shrinkage potential. Sample 5 with shrinkage values ranging from 5-10% indicates medium-quality soil with moderate shrinkage tendencies. In contrast, samples 2 and 6 with shrinkage values between 10-15% may be classed as poor-quality soils with high shrinkage potential. The plasticity chart categorizes the soil samples based on their plasticity and compressibility. Samples 1 and 3 are classified under CI, signifying inorganic clay with medium compressibility and plasticity (Fig. 4). Sample 4 is categorized as CL, which is indicative of inorganic clay with low compressibility and plasticity. Samples 2, 5 and 6 fall in the MI/OI field and represents inorganic silt, very fine sand, or organic clay of medium compressibility and plasticity.

Direct shear test results classify samples 2 and 6 as weak soils with low shearing strength and load-bearing capacity. Soil samples 1, 3, 4 and 5 indicate very low shearing and load-bearing capacities (Table 3). The slope material, predominantly consisting of soil and rock debris, is inherently fragile. The rocks are highly sheared, pulverized, and weathered (Fig. 2).

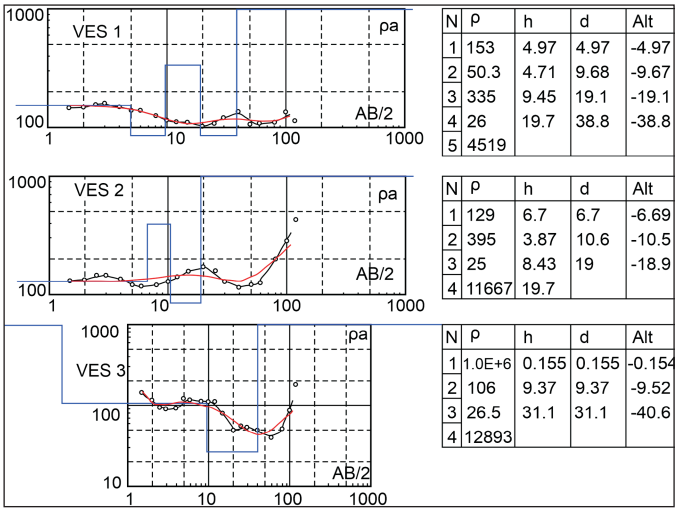

N	ρ	h	d	Alt
1	153	4.97	4.97	-4.97
2	50.3	4.71	9.68	-9.67
3	335	9.45	19.1	-19.1
4	26	19.7	38.8	-38.8
5	4519			

N	ρ	h	d	Alt
1	129	6.7	6.7	-6.69
2	395	3.87	10.6	-10.5
3	25	8.43	19	-18.9
4	11667	19.7		

N	ρ	h	d	Alt
1	1.0E+6	0.155	0.155	-0.154
2	106	9.37	9.37	-9.52
3	26.5	31.1	31.1	-40.6
4	12893			

Fig.6. Resistivity Curve chart

Slope mass rating classification for locations N1 and N2 suggests that the slopes in these locations are partially stable. However, they are susceptible to planar or wedge failure due to the numerous joints.

Results of kinematic analyses indicate planar mode of failure according to the Markland test (Markland, 1972). In slope N3, joint sets J1 (83° due 77°) and J3 (74° due 332°) intersect to produce a wedge with a NNE (2°) trend and the intersection between J2 (72° due 259°) and J3 produces a wedge trending WNW (290°).

It is considered a critical zone when the plunge of two intersecting discontinuities is less than the dip angle of the slope face but greater than the friction angle of the slope material (Hoek and Bray, 1981). According to structural orientations, all intersecting joints in the study area lie within the shaded portion representing the critical zone and thus prone to wedge mode of failure.

Based on the results obtained for VES 1, VES 2, and VES 3, the inferred subsurface layers at depths greater than 40 m and showing resistivity values greater than 4000 Ωm, may consist of more compact rocks with low moisture content and are considered undefined strata. Fractured and weathered shale, or shale with sandstone intercalations having resistivity values of 25-400 Ωm are found between the topsoil and the undefined strata at a depth exceeding 9 m. The topsoil and/or rock exposures found at shallow depths constitute the first layer. Here, the resistivity values range from 100-10000 Ωm. This may be due to the continuous ongoing weathering processes of the subsurface materials (Fig. 6; Table 5).

The analysis shows that the fractured rocks are weathered up to depths of about 40 m, suggesting the active role of subsurface water, which is noted in the wells of the study area. This protracted problem is, therefore, an outcome of a combination of various factors involving non-cohesive soils that tend to change state and shrink and swell with the abundance of moisture in the subsurface, weak weathered rocks, and the large number of intersecting joints that tend to cause wedge failure.

Conclusions

This slope stability study aims to assess the rocks and soils in the landslide-affected Tarliedzü area and the adjoining Kohima-Meluri highway. Detailed studies reveal that the instability of the study area is primarily due to excess water content. Poor drainage permits excessive percolation of surface water into the subsurface and renders the slopes weak and susceptible to failure. The weak, medium to highly plastic soils that form the lithology of the area, interact with moisture exacerbating the problem regularly. The soils

also possess low to very low shearing strengths and very low bearing capacities that are regarded as highly unstable and fail on excessive loading. Kinematic analyses and electrical resistivity data show that the area is predominantly made up of jointed, fractured, crushed, and weathered rocks. Water saturation of these soils and rocks causes a build-up of pore-water pressure and swelling of the slope material. The resultant subsurface drainage also carries away finer materials leading to subsidence in many parts of the area. The joint alignments of the rocks also induce a wedge-mode of failure under the action of gravity. Factors such as unscientific cutting of slopes for the construction of houses and roads, loading from the settlements, and vibrations due to heavy vehicles traversing the area cannot be ignored. The interplay of all these factors has led to the development of a weak zone in the study area that fails regularly as complex landslides.

These conditions underscore the challenges associated with slope stabilization and highlight the critical need for effective water management and soil stabilization strategies in the area. To reduce instability, the construction of well-designed drainage systems is imperative. Furthermore, given that the slope materials are predominantly composed of weak soil and rock debris, the construction of heavy structures should be avoided.

Authors' Contributions

NK: Investigation, Formal Analysis, Writing Original Draft, Methodology, Data Curation, Visualization, Reviewing and Editing, Software. **CNC**: Investigation, Formal Analysis, Methodology. **ME:** Investigation, Formal Analysis, Writing Original Draft, Methodology, Data Curation, Software. **GTT**: Investigation, Formal Analysis, Reviewing and Editing. **VK**: Investigation, Formal Analysis. **KD**: Investigation, Formal Analysis, Writing Original Draft. **KM**: Investigation, Formal Analysis. **TW**: Conceptualization, Investigation, Formal Analysis, Supervision, Reviewing and Editing.

Conflict of Interest

Authors declare no conflict of interest.

Acknowledgments

The authors are grateful to the Department of Geology, Nagaland University, for extending the laboratory facilities and equipment for the preparation of the paper.

References

Aier, I., Luirei, K., Bhakuni, S.S., Thong, G.T. and Kothyari, G.C. (2011). Geomorphic evolution of Medziphema intermontane basin and Quaternary deformation in the schuppen belt, Nagaland, NE India. Zeitschrift fur Geomorphol., v. 55, pp. 247-265. https://doi.org/10.1127/0372-8854/2011/0055-0048.

Alimohammadlou, Y., Najafi, A. and Gokceoglu, C. (2014). Estimation of rainfall-induced landslides using ANN and fuzzy clustering methods: a case study in Saeen Slope, Azerbaijan province, Iran. Catena, v. 120, pp. 149-162, 10.1016/j.catena.2014.04.009.

Bhattacharjee, C.C. (1991). The ophiolites of Northeast India: a subduction zone Ophiolite Complex of Indo-Burman Orogenic Belt. Tectonophysics, v. 191(3-4), pp.213- 222.

Bicocchi, G., Tofani, V., D'Ambrosio, M., Tacconi-Stefanelli, C., Vannocci, P., Casagli, N., Lavorini, G., Trevisani, M. and Catani, F. (2019). Geotechnical and hydrological characterisation of hillslope deposits for regional landslide prediction modeling Bull. Eng. Geol. Environ., v. 78, pp. 4875-4891, 10.1007/s10064-018-01449-z

Bieniawski, Z.T. (1989). Engineering rock mass classifications. New York: Wiley.

Bobachev, A. (2003). IPI2win-1D automatic and manual interpretation software for VES data available online: geol.msu.ru/ipi2win.htm.

Bureau of Indian Standards (1998). IS 8764: Method of determination of point load strength index of rocks.

Bureau of Indian Standards (1985). IS: 2720-5: Method of test for soils: Determination of liquid and plastic limit (Second Revision) (Reaffirmed 2006).

Bureau of Indian Standards (1972). IS: 2720-6: Method of test for soils: Determination of shrinkage factors (First Revision) (Reaffirmed 2001).

Bureau of Indian Standards (1970). IS: 1498: Classification and Identification of Soils for General Engineering Purposes.

Census of India (2011). Census of India.

Godio, A., Strobbia, C. and De Bacco, G. (2006). Geophysical characterisation of a rockslide in alpine region. Eng. Geol., v. 83, pp. 273-286**.**

Hoek, E. and Bray, J. (1981). Rock Slope Engineering, 3rd edn, Inst. Mining and Metallurgy, London, UK.

Hong, H., Chen, W., Xu, C., Youssef, A.M., Pradhan, B. and Tien Bui, D. (2017). Rainfall-induced landslide susceptibility assessment at the Chongren area (China) using frequency ratio, certainty factor, and index of entropy. Geocart. International., v.32(2), pp.139-154. doi.org/10.1080/10106049.2015.1130086.

Imchen, W., Thong, G.T. and Pongen, T. (2014). Provenance, tectonic setting, and age of the sediments of the Upper Disang Formation in the Phek District, Nagaland. Jour. Asian Earth Sci., v. 88, pp.11-27. https:// doi.org/10.1016/j.jseaes.2014.02.027.

Jongmans, D. and Garambois, S. (2007). Geophysical investigation of landslides: A review; Bull. Soc. Geol. France, v. 178(2), pp. 101-112, https://doi.org/10.2113/gssgfbull.178.2.101.

Kawabata, D. and Bandibas, J. (2009). Landslide susceptibility mapping using geological data, a DEM from ASTER images and an ArtiBcial Neural Network (ANN). Geomorphology, v. 113(1-2), pp. 97-109, https://doi.org/10.1016/j.geomorph.

Lapenna, V., Lorenzo, P., Perrone, A., Piscitelli, S., Rizzo, E. and Sdao, F. (2005). 2D electrical resistivity imaging of some complex landslides in Lucanian Apennine chain, southern Italy. Geophysics, v. 70(3), 10.1190/1.1926571.

Markland, J.T. (1972). A useful technique for estimating the stability of rock slopes when the rigid wedge sliding type of failure is expected. Imperial College Rock Mechanics Research Report No. 19,10, pp.13.

Morley, C.K., Tin Tin Naing, Searle, M., Robinson, S.A., Naing, T.T., Searle, M. and Robinson, S.A. (2020). Structural and tectonic development of the Indo-Burma ranges. Earth-Science Rev., v.200. https://doi.org/10.1016/j.earscirev.2019.102992.

Nandy, D.R. (1976). The Assam syntaxis of the Himalayas – A re-evaluation. Geol. Surv. India Misc. Pub. 24, pp. 363-368.

Orellana, E., and Mooney, H.M. (1966). Master tables and curves for vertical electrical sounding over layered structures. Interciencia, Madrid, 34p.

Palmström, A. (1982). The volumetric joint count - A useful simple measure of the degree of rock jointing, in: Fourth Congress, IAEG. Delhi, pp. 221-228.

Perrone, A., Zeni, G., Piscitelli, S., Pepe, A., Loperte, A., Lapenna, V. and Lanari, R. (2006). Joint analysis of SAR interferometry and electrical resistivity tomography surveys for investigating ground deformation: The case-study of Satriano di Lucania (Potenza, Italy); Eng. Geol.,

v. 88(3-4), pp. 260-273, https://doi.org/10.1016/j.enggeo.2006.09.016.

Ramakrishna, D. and Rajeshwara Rao, N. (2023). Geotechnical Investigation and Monitoring of Underground Excavation of Tunnel-2 in Srisailam Left Bank Canal Tunnel Project (AMRP), Nalgonda District, Telangana, India. Jour. Geosci. Res., v. 8(1), pp. 18-24.

Romana, M. (1985). New adjustment ratings for application of Bieniawski classification to slopes, in: Proceedings of the International Symposium on the Role of Rock Mechanics in Excavations for Mining and Civil Works. International Society of Rock Mechanics, Zacatecas, pp. 49-53.

Song, S. and Wang, W. (2019). Impacts of antecedent soil moisture on the rainfall-runoff transformation process based on high- resolution observations in soil tank experiments Water (Switzerland), v. 11, pp. 15-20, 10.3390/w11020296.

Saikia, Arupjyoti. (2020). Earthquakes and the Environmental Transformation of a Floodplain Landscape: The Brahmaputra Valley and the Earthquakes of 1897 and 1950. Environ. Hist., v. 26(1), pp. 51-77.

Singh, T.N., Kainthola, A., Venkatesh, A. and Venkatesh A. (2012). Correlation between Point Load Index and Uniaxial Compressive Strength for Different Rock Types. Rock Mech. Rock Eng., v. 45, pp. 259-264. https://doi.org/10.1007/s00603-011-0192-z.

Srivastava, Sanjai and Pandey, Nagendra. (2011). Search for Provenance of Oligocene Barail Sandstones in and around Jotsoma, Kohima, Nagaland. Jour. Geol. Soc. India, v. 77, pp. 433-442. 10.1007/s12594-011-0045-0.

Suraj, P.R., Melvin Babu., Manoharan, A.N., Archana Krishnan, N., Shruthi Mayya, K. and Niveditha, P. (2024). Landslide susceptibility modelling of Central Highland Part of Chaliyar River Basin, Kerala, India with integrated algorithms of frequency ratio and shannon entropy. Jour. Geosci. Res., v. 9(2), pp. 100-107.

Telford, W.M., Geldart, L.P. and Sheriff, R.E. (1990). Resistivity Methods. *In*: Applied Geophysics, 2nd Edition, Cambridge Univ. Press, Cambridge, UK, pp. 353-358. https://doi.org/10.1017/cbo9781139167932.012.

Verma, R.K. (1985). Geology and Tectonics of Indian Peninsula. In: Gravity Field, Seismicity and Tectonics of the Indian Peninsula and the Himalayas. Solid Earth Sci. Lib., v. 3. https://doi.org/10.1007/978-94-009-5259-1_2.

Wei, W., Fan, W.,Cao,Y., Chai, X., Bordoni, M., Meisina, C. and Li, J. (2020). Integrated experiments on field monitoring and hydro-mechanical modeling for determination of a triggering threshold of rainfall-induced shallow landslides. A case study in Ren River catchment, China Bull. Eng. Geol. Environ., v. 79, pp. 513-532, 10.1007/s10064-019-01570-7.

Yang, J., Dai, J., Yao, C., Jiang, S., Zhou, C. and Jiang, Q. (2020). Estimation of rock massproperties in excavation damage zones of rock slopes based on the Hoek-Browncriterionand acoustic testing. Int. Jour. Rock Mech. Min. Sci., v. 126, 104192. https://doi.org/10.1016/j.ijrmms.2019.104192.

Zuoan, W., Shihai, L., Wang, J.G. and Ling, W. (2006). A dynamic comprehensive method for landslide control. Engineer. Geol., v. 84(1-2), pp. 1-11.